E-proceedings of the 36th IAHR World Congress
28 June – 3 July, 2015, The Hague, the Netherlands

# ACOUSTIC MAPPING VELOCIMETRY PROOF-OF-CONCEPT EXPERIMENT

MARIAN MUSTE[1], SÁNDOR BARANYA[2], RYOTA TSUBAKI[3], DONGSU KIM[4], HAO-CHE HO[5], HENG-WEI TSAI[1], DANIELLE LAW[1]

[1] *IIHR-Hydroscience & Engineering, The University of Iowa, Iowa City, IA 52242, IA, USA, marian-muste@uiowa.edu*

[2] *Department of Hydraulic and Water Resources Engineering, Budapest University of Technology and Economics, Budapest, H-1111, Hungary,*

[3] *Civil and Environmental Engineering, Hiroshima University, Higashi-Hiroshima, Japan, rtsubaki@hiroshima-u.ac.jp*

[4] *Civil and Environmental Engineering, Dankook University, 126 Jukjeon-dong, Yongin-si, Geyonggi-do, South Korea, dongsu-kim@dankook.ac.kr*

*baranya.sandor@epito.bme.hu*

[5] *Institute of Physical Oceanography, Ocean College, Zhejiang University, 310058, Hangzhou, China, howard-ho@zju.edu.cn*

## ABSTRACT

Knowledge of sediment dynamics in rivers is of great importance for various practical purposes. Despite its high relevance in riverine environment processes, the monitoring of sediment rates remains a major and challenging task for both suspended and bedload estimation. While the measurement of suspended load is currently an active area of testing with non-intrusive technologies (optical and acoustic), bedload measurement does not mark a similar progress. This paper describes an innovative combination of measurements techniques and analysis protocols that establishes the proof-of-concept for a promising technique, labeled herein Acoustic Mapping Velocimetry (AMV). The technique estimates bedload using non-intrusive measurements acquired in rivers developing bedforms.

The raw information for AMV is collected with acoustic multi-beam technology that in turn provides maps of the river bathymetry over swaths of the river cross-section (acoustic mapping). As long as the acoustic maps can be acquired relatively quickly and the repetition rate for the mapping is commensurate with the movement of the bedforms, the acoustic maps can capture continuously the progression of the bedform movement. Conversion of the bed elevation maps in homologous gray-level "images" followed by application of particle image velocimetry concepts to the obtained maps allow quantification of the bedform dynamics as two-dimensional velocity maps superposed on the streambed plane. Furthermore, use of the velocity fields in conjunction with conventional analytical methods for estimation of the bed movement (e.g., Exner equation) enable estimation of bedload rates over the whole imaged area in any direction. The technique represents a promising approach for in-situ measurement of the bedform dynamics either as a distribution of bedload rates over the stream cross section or as a bulk bedload rate in the streamwise direction, as typically requested in most of the practical applications.

*Keywords*: image velocimetry, large-scale particle image velocimetry, acoustic mapping, bedform dynamics, bedload transport

## 1. INTRODUCTION

Knowledge of sediment dynamics in rivers is of great importance for several practical applications. Sediment movement on the bed (i.e., pick-up, rolling, and deposition of sediment grains) has direct influence on aquatic ecosystems, fluvial navigation, hydropower, or water supply. Despite the importance of sediment-related problems in riverine environment monitoring sediment transport (suspended or bedload) remains a major issue for river engineers and geographers mainly due to the challenges of the measurement process. This paper focuses on the detection of the dynamics of bedform migration, which is the dominant sediment transport mechanism in sand bed rivers. The bedload transport can be defined as the movement of sediment particles in a thin layer, about two particle diameters thick above the bed, by sliding, rolling, and short-time sediment grain entrainment over a few diameters (Einstein, 1942). The local measurement of bedload transport rate with conventional sampling methods, such as pressure-difference samplers (e.g., Helley and Smith; 1971), is expensive both with respect to time and cost as the significant spatial and temporal bedform variability requires a large number of samples. Moreover, the intrusive nature of the grab and sample measurement methods questions the accuracy and representativeness of the measurement as a whole.

Given the limitations of the direct sampling methods, alternative measurement approaches are increasingly used to monitor bedload transport (Gray et al., 2010). Among the most popular methods are the acoustic Doppler current profilers (e.g. Rennie and Millar, 2004) and sonars (Holmes, 2010). These methods are labeled as surrogates by Gray et al. (2010) and defined as: "Instruments coupled with operational and analytical methodologies that enable acquisition of temporally and (or) spatially dense fluvial - sediment data sets without the need for routine collection and analysis of physical samples other than for periodic calibration purposes". These methods utilize the measurement of a virtual bedload velocity that in conjunction with a known bedload layer thickness can provide estimates of bedload rates (e.g., van Rijn, 1984). The thickness of the bedload layer can be estimated with empirical formulas involving a physical bed-material parameter (e.g.,

$d_{50}$, $d_{90}$) and additional coefficients obtained empirically (Einstein, 1942) or analytically (Pal and Ghoshal, 2014). Considered herein is the popular Exner bedload estimation method that requires the bedform migration velocity as input. The method further assumes that the bedform can be described as a uniform two-dimensional shape (i.e., triangular) propagating downstream. Conventionally, the bedform migration velocity is estimated by observing the dune height variation at one point on the bed (e.g., Abraham and Kuhnle, 2006). Alternatively, there are approaches that determine the velocity of the dune crest directly (Rubin et al., 2001). Given that bedforms are highly variable across the cross-section in terms of dune length, migration velocities provided by direct velocity measurement approaches would be more realistic.

This paper reports on proof-of-concept experiments conducted with a new measurement technique that combines components and processing protocols from two contemporary nonintrusive instruments: acoustic and image-based. The bedform mapping is conducted with acoustic surveys while the estimation of the velocity of the bedforms is obtained with processing techniques pertaining to image-based velocimetry. Given the combination, we call the technique acoustic mapping velocimetry (AMV). The implementation of this technique produces a whole-field velocity map associated with the multi-directional bedform movement. The paper demonstrates that the non-intrusive AMV technique has capabilities to: a) track the dynamics of the bedforms in the two-dimensional space, and b) provide rates of bedload motion in multiple directions. Currently, the techniques can be applied to both laboratory and field conditions as the acoustic mapping technology benefits from a wide range of instruments to choose from.

## 2. AMV METHODOLOGY

Irrespective of the targeted AMV measurement outcome, the implementation of the AMV concept entails two phases. In the first step the acoustic maps are created as a continuous depth-data layer covering the target area of the channel bottom. In the second step, the acoustic maps are converted to an "image-equivalent" through resampling of the raw information. The obtained images are subsequently processed with image velocimetry techniques. Bedload rates are obtained by combining the outcomes from both acoustic mapping acquired in step 1 and the velocity fields obtained in step 2 with analytical relationships. Brief overview on the background of steps 1 and 2 are provided below.

**Creation of bedform acoustic maps.** Acoustic maps are 3D representations of the bed geometry. The maps can be created using different instruments depending on the measurement situation. For field studies, single beam and multibeam echo sounders (MBES) or acoustic Doppler current profilers can be used for acquiring the maps (Spasojevic and Muste, 2002). Single beam echo sounders and the ADCP provide depth information along lines (tracks), whereas MBES surveys result in multi-lines that can be easily converted to surfaces of bed elevations with significantly higher resolution than the former methods. For laboratory experiments, detection of bed changes can be carried out with ultrasonic bed profilers equipped with a single sensor or bundled sensor arrays. Similarly to MBES, the array of sensors are more proficient as they allow scanning with multiple points (Ho et al, 2012). Regardless of the instrument used and measurement situation, the acoustic sensors output a cloud-like dataset of bed-elevation points replicating the shape of the bottom of the water body during the survey. If sampled with sufficient density, the discrete depth values acquired by each sensor can be interpolated to lend a map of the channel bottom.

Irrespective of the experimental situation (i.e., laboratory or field conditions), there are important considerations that need attention prior to mapping with acoustic survey instruments. Similarly to the recording of a photographic snapshot (whereby all the image pixels are captured at the same instant), the acoustic map should ideally contain depth measurements acquired simultaneously over the whole mapped area. This is however impossible to attain using instruments that construct the map by scanning the target area with individual sensors or (at best) with sensors arranged as arrays of finite length. Given that the depth measurements are not acquired simultaneously, the obtained map will be unavoidably affected by the movement of the bedform during the acquisition of the depth measurements. For a better understanding of these implications, a linear array of acoustic sensors as used in the present experiments is discussed below (see Figure 1).

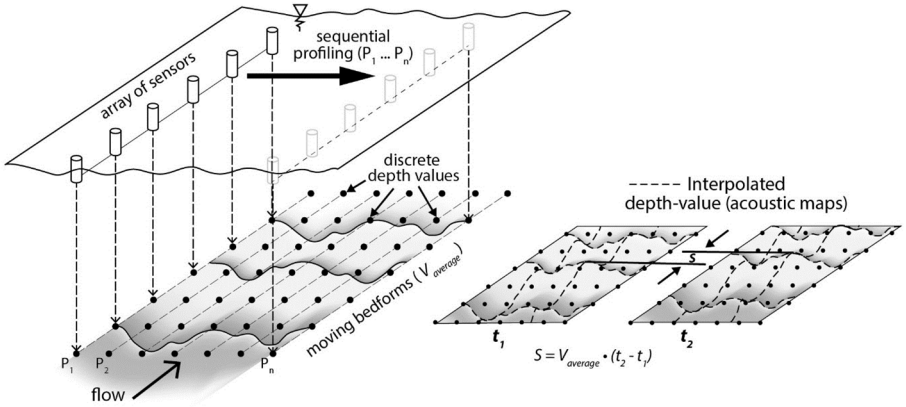


Figure 1. Schematic of the process leading to the creation of acoustic maps using an array of acoustic sensors.

The mapping with a linear arrangement of the sensor array is initiated on one side of the area to be measured. To attain a prescribed accuracy of the depth measurements at each location there is a need to average over a number of repeated depth readings. The number of repetitions is related to the accuracy and sampling frequency of the depth instrument used in the survey. For laboratory conditions for example, the sampling duration for one location is of the order of 1-2 seconds

for a medium quality acoustic sensor. The sensor array is successively positioned over the area targeted for mapping using the same protocol for each location. Closer spacing between successive locations yields better resolution in sampling the fine structure of the bedforms. The sequential measurement and relocation of the sensor array take a certain amount of time for covering the entire area targeted by mapping. Given that during the sweep the bedforms continue to progress, the map assembled using the above protocol will unavoidably combine information about the bedform taken at different times. Given this complex combination between the limited capabilities of the instrument data acquisition procedure, there are tradeoffs that the operator has to make in order to attain good accuracy and realistic mapping. The main choices that an experimenter have is to shorten the time required for mapping or to reduce the area to be mapped to a size that is manageable for the available instrument and measurement protocol.

In summary, the accurate construction of the maps require development of a measurement protocol that gives full consideration to the characteristics of the instruments, the size of the target map, the time needed to relocate the sensor(s) over the measured area, and the bedform geometry to be mapped and their dynamics. As intriguing as it sounds, the last consideration needs to be known even before conducting the mapping. From this perspective, before acquiring acoustic maps in a new situation, preliminary measurements should be acquired to roughly assess characteristics of the bedforms (e.g., dune wavelength, other geometrical characteristics) and their dynamics. Based on these preliminary measurements, the spatial coverage of the measurement and the associated protocols can be accordingly adjusted. Once acquired, the acoustic maps are typically presented as color-coded or iso-contour maps. The color maps are 2.5-dimensional representations of the domain, whereby the range of colors represent the bed elevation.

**Estimation of the bedform velocity maps.** The idea of observing bedform dynamics from acoustic maps is inspired by particle image velocimetry concepts (Adrian, 1991). Essentially, image velocimetry estimates probable displacements of recognizable patterns embedded in a sequence of images. The displacements are determined using a statistical approach whereby a pattern matching technique is applied to image intensity distribution in a series of images (Adrian, 1991; Fujita et al., 1998). The analysis is made successively over the entire imaged area using small interrogation areas (IA) covering the area subjected to measurement, as illustrated in Figure 2a. The similarity index for patterns enclosed in a small IA in an image is calculated for the same-size window within a larger Search Area (SA) selected in the subsequent image. The selection of IA and SA is guided by heuristic rules of thumb (e.g., Adrian, 1991; Raffel et al., 1998) but typically they are optimized by trial and error for a given application.

The similarity index used for image processing in this paper is estimated using the spatial cross-correlation (Fujita et al., 1998) applied to a pair of acoustic maps (shown in figure 2.b). Fujita's algorithm is based on an image velocimetry approach developed by Fincham and Spedding (1997) that is favorable for this application as the cross-correlation is applied to grey-level patterns in the image rather than point clusters (Muste et al., 2008). The Fincham and Spedding algorithm is similar to the cross-correlation algorithm applied to linear seafloor features embedded in the acoustic maps developed by Duffy (2006). The result of image velocimetry processing is a distributed velocity field uniformly covering the acoustically mapped area (see Figure 2.c).

Prior to applying image velocimetry to acoustic maps, the conversion of the acoustic maps to gray-level maps is needed. For this purpose, the depth measurements obtained as described above and color-mapped using red, green and blue are converted into gray-colored pixels using a scale from 0 to 255. The interpolated color maps are converted in pixel coordinates by successively sampling the entire image. The resolution of the pixel image is decided by the user, but it should be commensurate with the spatial resolution of the mapping and the scale of the bedform spatial features. The technique as described herein is well suited for both field and laboratory conditions. In this paper, we used a series of laboratory measurements acquired in a moving-bed open-channel flow experiment to illustrate the feasibility of the AMV concept. The use of AMV as described herein provides a wealth of information that is difficult (if possible at all) to obtain with any other alternative measurement approach.

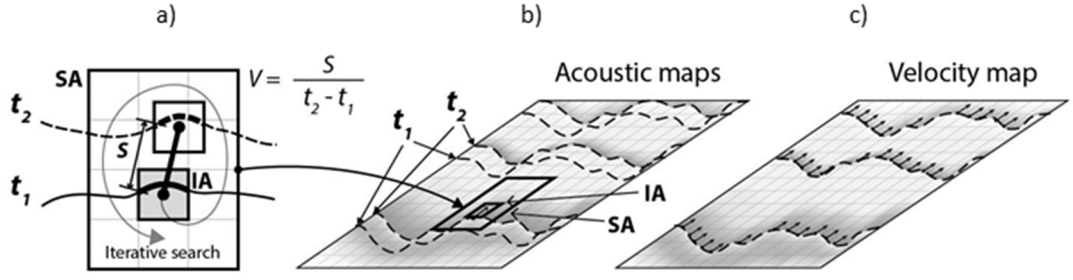


Figure 2. Schematic of the image velocimetry process: a) selection of the search and interrogation areas; b) implementation of the pattern matching over the image containing identifiable patterns; c) results of the image velocimentry applied over the whole image.

**Quantification of the bedload rates.** The whole-field velocity distribution associated with acoustic maps can be used in in conjunction with analytical methods for evaluating bedload rate estimates. The method selected for this study is based on the continuity equation applied to bedform movement (Exner, (1925):

$$(1-p)\frac{\partial y}{\partial t} + \frac{\partial q_b}{\partial x} = 0 \qquad [1]$$

where $p$ = porosity of the river bed, $y$ = bed elevation, $t$ = time, $q_b$ = volumetric bedload transport rate per unit width and $x$ = longitudinal distance. Assuming a steady uniform flow and that the dunes are in equilibrium, Simons et al. (1965) introduced the following formula for the volumetric bedload per unit width:

$$q_b = (1-p)V_D\frac{\Lambda}{2} \quad [2]$$

where $V_D$ is the bedform velocity and $\Lambda$ is the bedform height. The bedload transport by weight can then be estimated by multiplying $q_b$ by the density of the sediment and integrating it along the given cross-section of the river.

The estimation of bedload rates using Equation (2) entails the following steps:

1. acquisition creation of a sequence of acoustic maps (preferably at equal time steps).
2. quantification of bedform dynamics (i.e. calculation of 2D bedload velocity fields within the mapped area)
3. Determination of characteristic bedform height within the mapped area
4. estimation of bedload transport using Equation (2) in conjunction with information obtained in steps 2 and 3

A practical illustration of the Exner equation implementation using AMV measurements is provided next.

## 3. EXPERIMENT

***Facility and instrumentation***. A 6-m long, 0,75-m wide, and 0.40-m deep adjustable slope channel located at IIHR-Hydroscience & Engineering (IIHR) was used for conducting the experiments (see Figure 3). Structural steel frame members provided ample support along the model test section to avoid deflections in the roadway and curb surfaces. The channel was fed with water through a multi-hole diffuser set in the channel headbox. Inflows to the model were measured with a calibrated orifice meter with stated accuracies of ± 3% of reading. The flow meter was installed to ANSI standards. Provisions were made at the channel entrance to condition the flow and increase its turbulence intensity. For this purpose, a series of bluff blocks were set on a thick perforated mat as shown in the figure. Water level was controlled by an adjustable gate set at the channel end. Flow uniformity during the tests was checked using a point gage. Depth readings were acquired at five locations along the channel with periodic repetition to ensure that the flow uniformity is maintained. During the experiments the slope was adjusted using a set of removable vertical support legs and a pillow block bearing at the downstream end of the channel. During the experiments the channel slope was set at 1%, while discharge varied in the 0.01- 0.04 $m^3$ range. The hydraulic specifications for the experimental runs reported in this paper are provided in Table 1.

Well-sorted course sand with $d_{50}$=0.6mm and $d_{mean}$=0.77mm was used as bed material. This sand type was successfully used for several previous modeling studies on bedload transport (e.g., Muste and Ettema, 2000; Ho et al., 2013). A sand layer, 0.05-m thick, was set on the channel bottom throughout its length. The sand bed was leveled at the beginning of each new experimental run. At the downstream end of the channel a sediment trap was placed. The final sediment trap volume and interior shape was established using a trial and error approach. The tests were aimed at trapping all the sediment coming out from the channel to accurately quantify the sediment transport in the facility. The tests were conducted over long time intervals and over the whole range of discharges used on the experiments. Following each experimental run, the trapped sand was collected, oven-dried and weighed for estimating transport rates for the bedload.

The bathymetric measurements reported in this paper were acquired in a laboratory setting using a SeaTek Multiple Transducer Array (MTA). MTAs are suitable for bathymetric surveys both in field and laboratory environments (http://seatek.com). The MTA sensors measure depth using high frequency sound pulses. The travel time principle is at the basis of MTA operation. Specifically, sound wave pulses are transmitted toward the bed where the waves are partially reflected back to the sensor. The sensor records the time for the sound waves to travel from the sensor to the object and back to the sensor. Using the speed of sound in the medium and the recorded travel time of the pulse, the distance from the sensor to the reflective object is estimated, which is then converted into bed elevation reported in the instrument's coordinate system. The relevant characteristics of the MTA individual sensors used in the present study are summarized in Table 2.

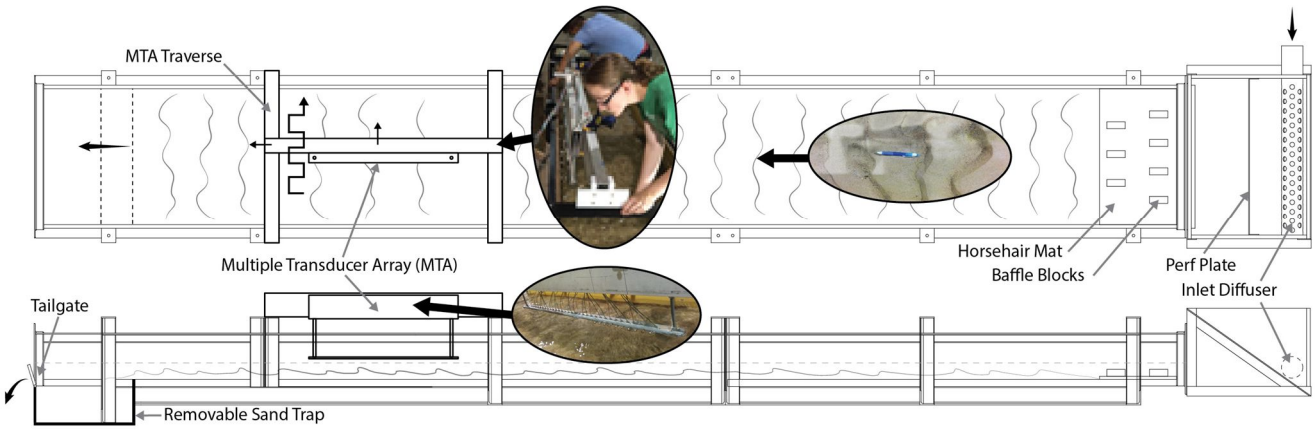


Figure 3. Schematic of the experimental flume, MTA arrangement, and measurement protocols

Table 1. Flow specifications for the proof-of-concept experimental runs

| | ***Discharge*** ***Q*** **($m^3/s$)** | ***Width flume*** ***B*** **(m)** | ***Flow depth*** ***H*** **(m)** | ***Mean velocity*** ***U*** **(m/s)** | ***Fr*** |
|---|---|---|---|---|---|
| **RUN 1** | 0.0227 | 0.762 | 0.1 | 0.30 | 0.30 |
| **RUN 2** | 0.0198 | 0.762 | 0.095 | 0.27 | 0.28 |
| **RUN 3** | 0.0181 | 0.762 | 0.09 | 0.26 | 0.28 |

This instrument has been successfully used for bathymetric measurements in previous laboratory shallow flows by Friedrich et al. (2005), Abraham and Kuhnle (2006), and Lin (2011). The sensor array manufacturer provides a DOS-based data acquisition package, which outputs an ASCII file containing raw bathymetry measurement and time stamps. However, no MTA-associated post-processing software is currently available for processing the dynamics of the measured bathymetric profiles. A customized plug-in software for the MTA was developed for this study to ingest the depth measurements in a customized processing database.

Table 2. MTA specifications (www.seatek.com)

| **SeaTek MTA System** | |
|---|---|
| **OPERATING FREQUENCY** | 5 MHz |
| **TRANSDUCER DIAMETER** | 0.01 m |
| **DEPTH RANGE** | 0.03 – 1.10 m |
| **MAX SCAN RATE** | 0.2 sec |

***Experimental protocol.*** The variables measured for controlling the flow conditions during the experiments included: water depth at several locations, incoming discharge, volumes and weight of trapped sand, and temperature. In addition to the above, measurements with the MTA were acquired using a protocol separately described below. Prior to each production test, an extensive number of runs were conducted to ensure the flow and bedform uniformity and to determine the duration over which these conditions are maintained in the test section. Given that the purpose of the production test was to compare two alternative measurement techniques, rather than accurate replication of a bedload transport processes, the sediment was supplied by the eroded material in the upstream section of the channel. Before each production run, the flume was set up and run for an extended period of time (about one day) to reach equilibrium and create even distribution of the bedforms. The experiments were conducted the day after setting the equilibrium flow with a special protocol that replicated the flow leading to the bedform creation without disturbing the existing bedforms. During these tests it was found that the facility could sustain uniform transport rates for up to 8 hours by continuous erosion of the material in the upstream scour whole without visible non-uniform depositions along the flume. The volumes of bed scour, sand deposit immediately downstream the scoured area, and of the trapped material were all estimated to verify that the flow was in equilibrium for each run and replicable for the same hydraulic conditions. Visual inspection and point gage measurements of the bed in the test section were made to verify that the test section is in equilibrium throughout the experiment. A view of the bed in the test section during the three production tests is provided in Figure 4.

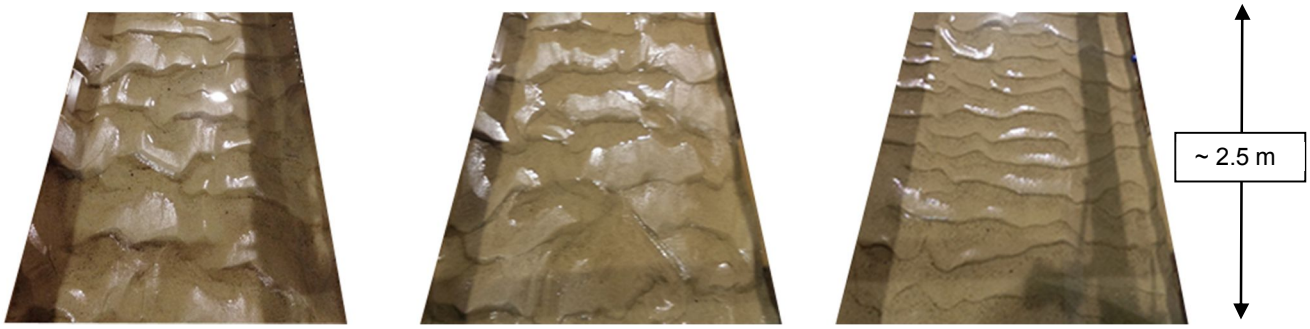


Figure 4. Photos of the bedforms obtained in Runs 1, 2 and 3. Flow from top to bottom.

The mapping was made with a MTA containing 32 sensors spaced at 3 cm apart. The array of sensors, illustrated in Figure 3, was set on a traverse to allow precision control of its position in the streamwise and spanwise directions. Motion of the MTA parallel to the flow was controlled with two clamps placed along the support beam upon which the MTA rested (one flush against one side of the MTA, and the other 1.5 cm from the opposite side). Motion perpendicular to the flow was quantified and controlled visually by two measuring tapes attached to the cross bars that the support beam rested on, as illustrated in Figure 3. Mapping of the bedforms started with the MTA positioned on the same side of the flume for each trial (see Figure 3 and 5). Once the MTA had finished sampling at the first position (up to 2 seconds), it was moved to the next position, 1.5 cm in the downstream direction, and the bedform heights were sampled again. From this position, the array was slid to a new position 1.5 cm away in the transverse direction. Thus a ladder pattern was established as the MTA moved across the flume as shown below, which yielded a resolution of roughly 1.5 cm × 1.5 cm. The

Each bed elevation point was sampled for 1 to 2 seconds at 5 Hz. The sampling time was established through preliminary tests to account for the probe accuracy and noise level in individual measurements. The side-to-side travel time for the MTA took 10 minutes to complete. The bedform movement during the 10-min travel inherently induced a continuous distortion in the mapped bedform from the position and shape at the time of the initiation of the mapping. The largest distortion, occurring between the starting and ending sides of each map, was assessed with video recordings at about 1.5 cm. Given this inherent measurement method limitation, it was critical to keep the mapping time strictly constant for all the acquired maps such that the distortion of each map would be similar. Despite the rigorous measurement protocols,

additional provisions were taken in processing to further minimize the distortion effects. A 10-minute break was taken following each map, followed by another mapping. No less than five consecutive maps were acquired for a given target flow rate.

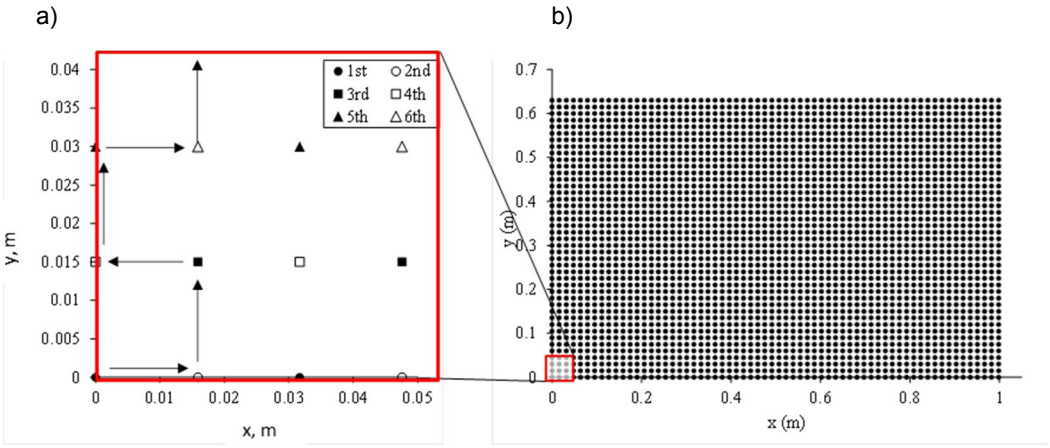


Figure 5. Creation of the acoustic maps: a) stepwise arrangement for collection of the depth measurements (the arrows on the left side of the figure trace the progression of one MTA sensor during the mapping); b) the depth measurement points for one mapping of the test area.

## 4. BEDLOAD ESTIMATION

### 4.1. Building of acoustic maps

Three sets of experiments were carried out at three different flow discharges. The flow depth at the outlet section was kept constant for each run with an average value of 0.1 m. The flow discharges for Runs 1, 2 and 3 were 0.0227 $m^3$/s, 0.0181 $m^3$/s and 0.0198 $m^3$/s, respectively. The measurements were performed at uniform flow conditions which were checked with water surface profiling and visual observations. During preliminary tests it was be observed that it took about one day of continuous flow over the sand-bed flume to bring the original flat bed to dynamic equilibrium conditions with fully-developed bedforms. The bedform mapping started the next day after attaining the equilibrium, using a carefully controlled protocol. The equilibrium was verified by periodically checking the amount of bed material that was retained in the sand trap. Another indicator of the status of the bedforms was visual observation of the bed which at equilibrium entailed well-defined bedforms with similar characteristics all along the test area. Five acoustic maps were subsequently acquired for each production run. The maps were acquired in the flume test section and are 1.0-m long and 0.64-m wide, as illustrated in Figure 6.

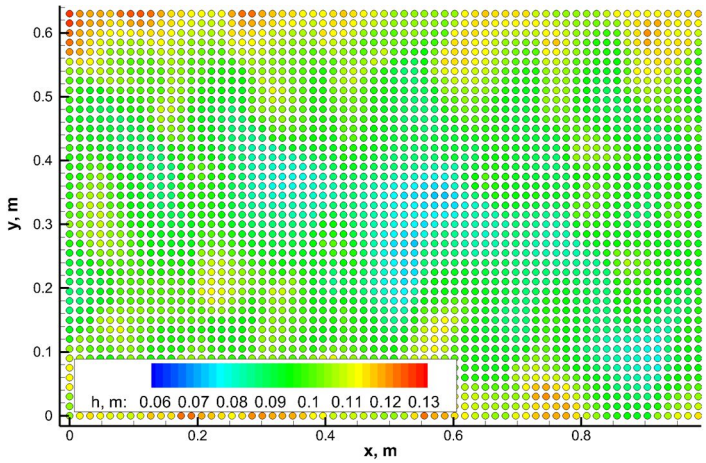


Figure 6. Example of an acoustic map created from the MTA scanning (run 1, first map).

### 4.2. Converting maps to images

The image processing software is applied to raster images, therefore the scatter points provided by the multi-array bed scanning method had to be converted into images. The transformation entails two steps. In the first step, the scatter points are triangulated to get a continuous surface of the flume bed. For this purpose, a linear interpolation is applied to obtain depth information between points with measured depth values. The depths were converted to grey-level contour images, as illustrated in Figure 7. Light gray zones indicate deep bed areas (low elevations) while dark patches indicate shallower flow areas (higher bed elevations). In the second step, the optimal resolution of the acoustic images is determined considering two aspects: i) to attain a reasonably fine resolution that is accurately replicating the bedform geometry, ii) to

limit the output image size as the computational demand of the processing software increases with the pixel number. Subsequent to several preliminary tests, the optimum pixel size was found to be 0.003m. This pixel resolution was uniformly applied for all acoustic mapping conversions.

Five acoustic maps were generated for each experiment. The time intervals between the maps was about 20 minutes. For illustration purposes, four grey-level acoustic maps from the first experiment are provided in Figure 7. The maps allow forobservation of the 3D bedforms developed along the flume with a characteristic wave length of ~0.20 m and a trough-to-crest height of ~0.02 m. The obtained images are characterized by adequate spatial resolution as the characteristic parts of the bedforms can be clearly distinguished, such as the stoss face, the crest, lee face and trough. The images show that a narrow area along the flume walls displays overall deeper flows compared to the central area where the opposite can be observed. The difference is attributed to the flume artifacts. Specifically, the presence of the wall induces additional stresses that enhance the sediment transport locally. This artifact does not affect the results of the experiments, as the goal of the validation experiment presented herein is to capture the cross-sectional bedload transport, similarly with what is targeted in field conditions.

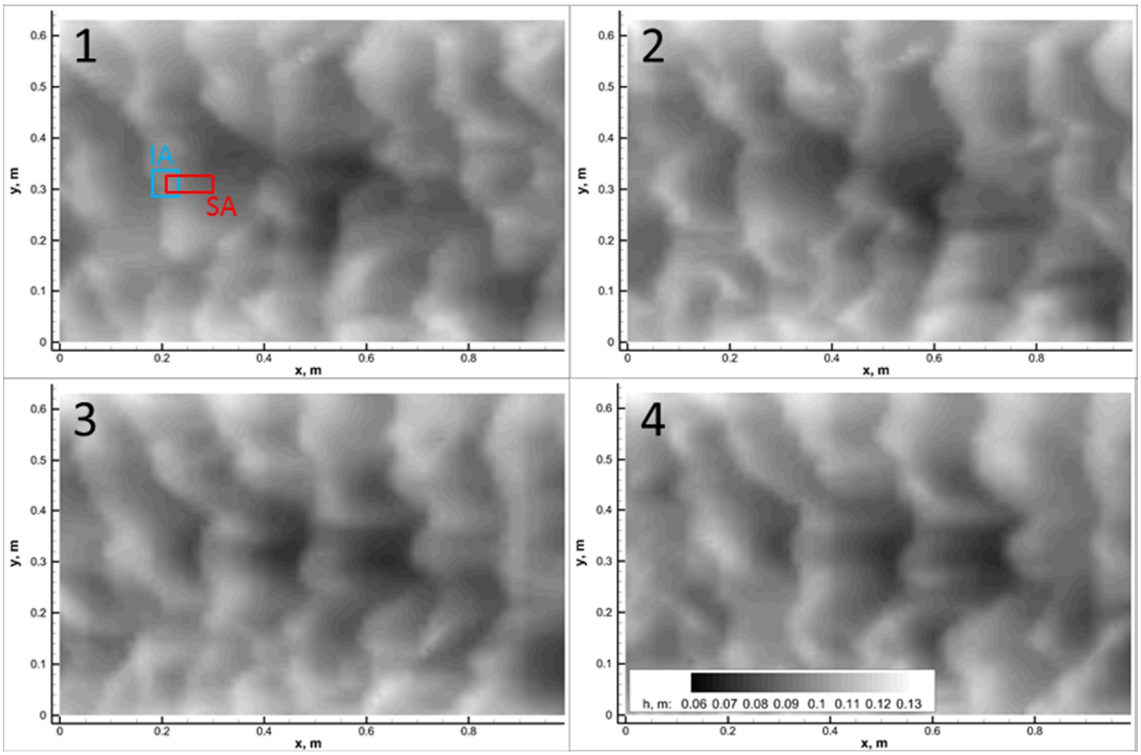


Figure 7. A sequence of grey-level acoustic images for Run 1.

4.3. Quantification of the bedform morphodynamics

Using the maps generated above, an image velocimetry procedure was applied to quantify the displacement of identifiable bedform features within pairs of acoustic maps recorded at successive times. The image processing software applied for processing is the Large Scale Particle Image Velocimetry (LSPIV). LSPIV has extensively been used for estimation of free-surface velocity distributions in rivers (e.g., Muste et al., 2008). The optimum sizes for the interrogation area (IA) and search area (SA) were selected based on a trial-and-error tests conducted before to process the acoustic maps obtained from the experimental runs. Use of large areas for these parameters smoothen out the spatially heterogeneous information while the use of small values for the parameters result in poor cross-correlation coefficients that are quality indicators for the image processing algorithm and used in the software as a filtering criterion. The preliminary tests suggested that the use of an interrogation area of 0.06x0.06 m and a search area of 0.03x0.09 m is optimal for the current situation. Frame 1 in Figure 7 displays the actual sizes of the SA and IA superposed onto the bed image.

The application of the image velocimetry procedure quantifies the bedform migration with associated velocity maps. Sample results of LSPIV processing applied to the acoustic maps are shown in Figure 8 where the velocity distribution superposed on the color-coded map of velocity intensity (as iso-contours) is shown using the first pair of images from Run 1. The figure plots the velocity vectors for a spatial resolution of 0.005 m. Zones without velocity vectors represent areas where the correlation coefficient is poor hence the results are filtered out. If suitable, interpolation schemes can be used to fill in the missing vectors. The range of the velocities for this flow condition is between $5{\cdot}10^{-6}$-$6{\cdot}10^{-5}$ m/s or 0.018-0.216 m/hour. The velocity iso-contours show a non-homogeneous vector field that is associated with both the non-homogeneous spatial distribution of the bedforms across and along the channel as well as with the flume-induced effects mentioned above.

The 2D velocity maps obtained with LSPIV software represent significant progress compared to earlier studies where bedform velocities are estimated along a line of sight orientated in the streamwise direction. The associated assumption with this measurement approach is that the bedform migration is unidirectional. While the assumption is valid for most parts of the area illustrated in Figure 8, there are, however, many subareas of the map where the flow is not fully aligned

with the streamwise direction. This is also expected, as the direction of the flow is dictated by the orientation of the bedforms that also show a quasi-2D distribution in Figure 7. The vector field plotted in Figure 8 illustrates that the bedform velocities are two-dimensional revealing a reasonable complexity. The capability of the LSPIV to estimate 2D velocity fields is important for natural rivers where we expect a large spatial non-homogeneity of the bedform orientation and geometry across the section.

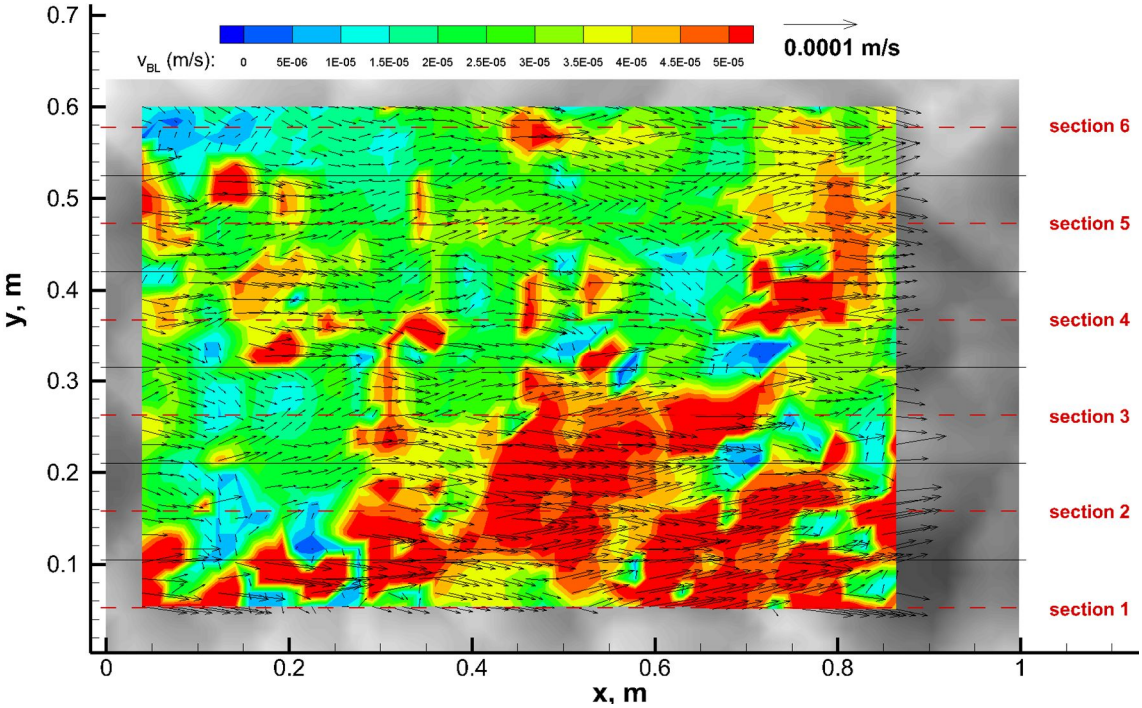


Figure 8. Bedform velocities estimated with image velocimetry software applied to the first image pair of acoustic maps acquired in Run 1. The longitudinal swaths (aligned in the streamwise direction) defined in the figure are used for checking the flow conditions and estimation of the bedload transport rates.

Section 3 of this paper revealed some challenges in acquiring acoustic maps using scanning of the mapping area with the acoustic array. It was mentioned that due to the instrument and measurement protocols limitations, mapping is affected by the movement of the bed. Verification of the impact of the moving bed on the accuracy of the velocity is tested herein by using a customized analysis as a resource. The analysis hypothesis is that during the hour-long acoustic mapping, the flow field was quasi-steady and bedforms were in equilibrium. To test the hypothesis, the test section was divided into six longitudinal swaths indicated as sections 1, 2, 3, 4, 5 and 6 in Figure 8. For each section, the mean velocity values were derived using only the streamwise component of the velocity. The so-obtained velocities using the 4 acoustic image pairs (1-2, 2-3, 3-4, 4-5) along with their average value for each section are plotted in Figure 9. The comparison of the distributions of individual velocities with their averages along the swaths indicates that, overall the average velocity spreading in the six areas is quite small, with higher variability in the central area where the depth is shallower. This confirms both the stability of the flow as well as the appropriateness of the measurement protocols.

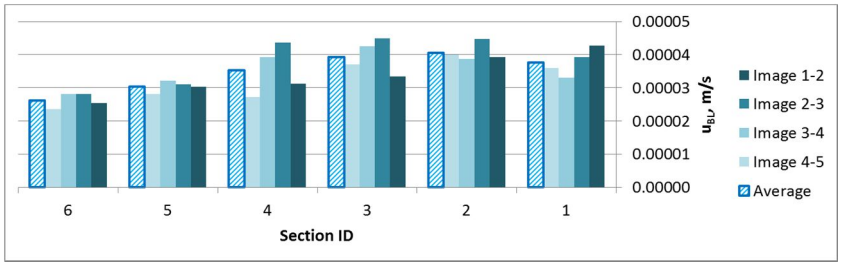


Figure 9. Cross-sectional distribution of mean bedload velocities for the six streamwise swaths forming the cross section in the acoustic maps acquired for Run 1

Similar analysis is conducted to assess the bedform homogeneity during the experiments. While the bedload velocity was analyzed using image pairs, the morphological characteristics of the bedform were obtained from the analysis of individual acoustic images. For the purpose of the latter analysis, the height of individual dunes ($H_i$) along the longitudinal sections is defined as the average of two measures (see Figure 10): i) distance from trough to crest, ii) distance from crest to trough. The so obtained average of the $H_i$ values provides the characteristic bedform height $\Lambda$, for each section. Besides being a characteristic geometrical parameter of the bedform, $\Lambda$ is a parameter needed for estimation of the bedload with the Exner equation. A sample of this calculation is provided in Figure 10a (for Section 1, in Run 1, first acoustic image). The distribution of $\Lambda$ for each of the six sections of image 1 from Run 1 along with the average of all $\Lambda$ values for the sections is plotted in Figure 10b. The distributions bundled for each section reflects the homogeneity of the bed geometry in the

streamwise direction and the stability of the flow during the 1.5 hour long experiment for acquiring the acoustic maps. The analysis reported here was conducted manually. However, these estimations can be also made using readily available tools such as the Bedform Tracking Tool of van der Mark et al. (2008).

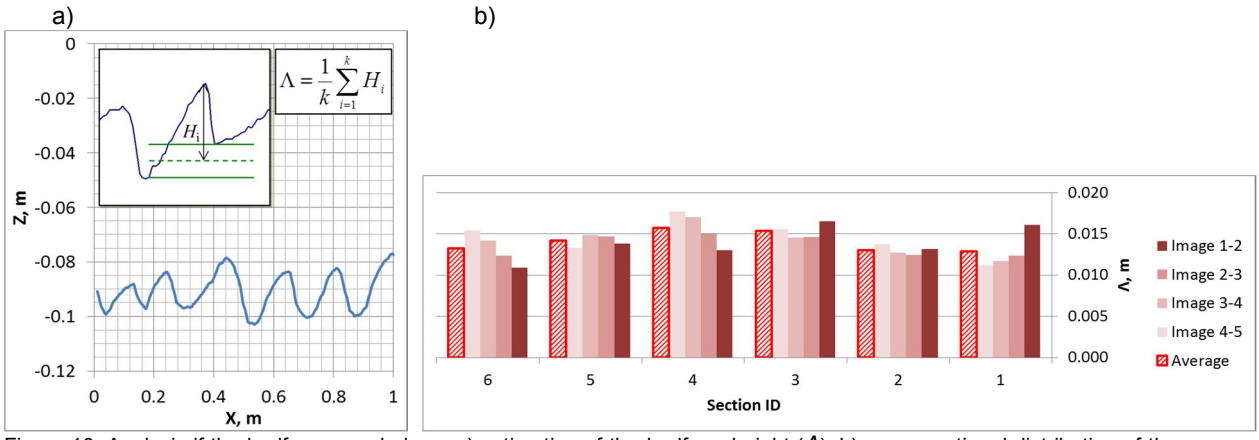


Figure 10. Analysis if the bedform morphology: a) estimation of the bedform height ($\Lambda$); b) cross-sectional distribution of the average and distributions of $\Lambda$ for the six streamwise swaths forming the cross section in the acoustic maps acquired for Run 1.

### 4.4. Bedload estimation

The formula for estimation of bedload in this paper is the Exner equation presented in Section 2. The equation is applied using bedload velocities obtained with image processing and bedform height using processing tools applied to the acoustic maps. None of the input for the equation is sampled empirically, rather they are obtained through direct measurements of moving bedforms acquired in real time. The only parameter that is based on prior information is the porosity of the bed material which was assumed $p$ = 0.4 as provided by Gibb et al. (1984). For the sake of simplicity no correction factor was applied for the bedform shape, i.e. the dune shape was assumed to be triangular. Alternatively, the bedform shape factor can be calculated using the form factor. The range of the variability of this factor is small as demonstrated by the study of Duffy (2006). Finally, the last parameter needed in the Exner equation is the density of sediment, evaluated as 2650 kg/m$^3$ for the sand used in the experiments.

Similarly to the velocity and bedform analyses discussed above, the bedload rates are determined for the individual streamwise swaths defined in Figure 8. The distribution of the individual bedload rates estimated for individual streamwise swaths for the image pairs of Run 1 along with the average bedload rates for the same areas are plotted in Figure 11. The distribution of the bedload rate estimates display slightly larger cross-sectional variability as a result of the combination of the individual scattering for the velocity and bedform geometry across the flume section. Nevertheless, the scattering does not obscure the clear inference of higher bedload rates in the central part of the flume compared with the deeper area along the walls. Also reflected in the distribution of the bedload rates in Figure 11 is the slight overall asymmetry of the flow transport across the channel. The variability of this, as well as of the other variables related to sediment transport discussed above, emphasize the good performance of the technique that is capable to capture details of the flow that are not available from measurements with other bedload instruments.

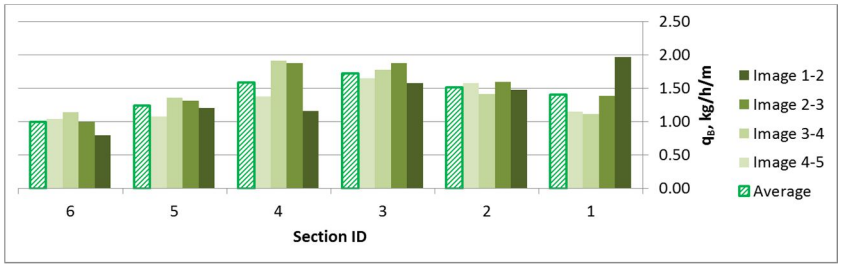


Figure 11. Distribution of bedload transport rates for the six streamwise swaths forming the cross section in the acoustic maps acquired for Run 1.

Irrespective of the measurement method, the bulk value for the mean bedload rate for a given flow discharge is the value of interest for practical applications. Using the dynamic and morphologic quantifications enabled by the AMV method, the bulk value of the bedload rate is estimated herein as the weighted average of the cross-sectional values obtained in Figure 11. The weights are commensurate with the streamwise swaths width. Due to the fact that MTA scanning cannot be acquired close to the flume sidewalls, the weights for the first and sixth swaths are higher. The estimated AMV-based bedload rates per unit width for all the runs of the reported experiments are summarized in Table 3 and plotted in Figure 12. These AMV bedload estimates are compared with the direct physical samples acquired with the sand trap in Table 3 and Figure 12. As can be noted from the comparison, the overall agreement between the physical samplings and the AMV based estimations are acceptable. The only exception is Run 2, where some experimental difficulties occurred in stability of the flow. The instability further affected the instantaneous rates of bedform migration, hence the long term average (8 hours) over which the physical samples were estimated might be different from the 1-hour long measurements for

constructing the acoustic maps that lead to the AMV bedload rate estimates. As a consequence, this run resulted in more scattering in all the variables.

Table 3. AMV-based bedload rates estimated for the experimental runs reported in the study

| | $Q$, $10^{-3}$ m$^3$/s | $q_{BL,\ sampled}$, kg/m/h | $q_{BL,\ AMV}$, kg/m/h |
|---|---|---|---|
| **RUN 1** | 22.65 | 1.37 | 1.36 |
| **RUN 2** | 19.82 | 0.62 | 0.99 |
| **RUN 3** | 18.12 | 0.33 | 0.44 |

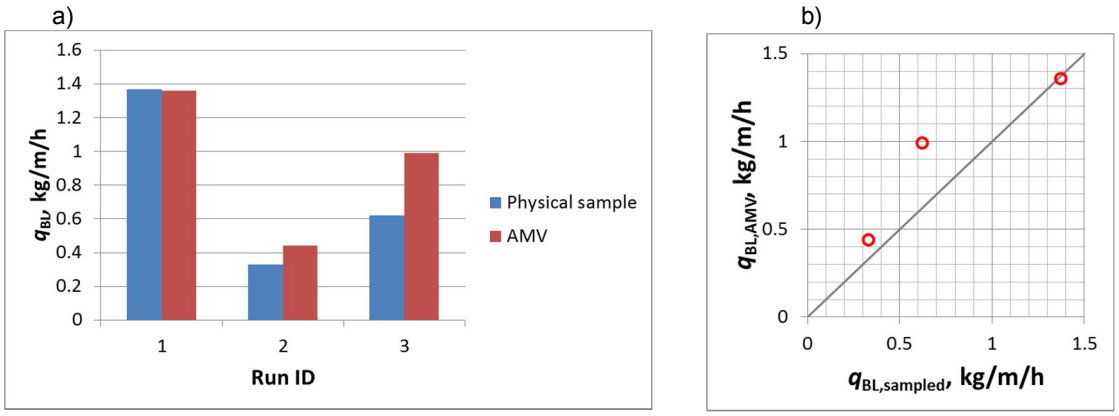


Figure 12. Comparison between bedload rates estimated with AMV and physical sampling: a) bar plot; b) agreement

## 5. CONCLUSIONS

The AMV methodology presented in this paper is a new and original measurement concept that integrates elements and techniques developed separately by various investigators over the time. AMV takes advantage of information available in the acoustic maps acquired non-intrusively with direct measurements. The technique distinguishes from the existing bedload estimation techniques as it does not require a priori assumptions of dune spacing, spatial distribution or celerity and is capable of determining directly other parameters needed in the analytical relationships leading to final results. Given the two-dimensional nature of the quantification of the bedform dynamics, the bedload rates can be estimated along multiple directions (i.e., from streamwise to spanwise). This makes AMV useful not only in riverine environments but also in coastal applications where the flow can be highly three dimensional.

The experiment presented in this paper illustrates the capability of AMV to qualitatively and quantitatively assess bedform dynamics. The end-to-end measurement protocol described in the paper is generic and it can be accomplished using a variety of technological, analytical, and visualization approaches. In essence, it assumes repeated recordings of a sequence of maps of the bathymetry in a moving body of water as a first step. Subsequently, image velocimetry concepts are applied to the acoustic images to infer quantitative information about the bedform migration and potentially other more complex features of the dune movement. The combination of techniques presented here takes advantage of recent advancement in acoustic and image technologies and it can be asserted that its development is a result of their capabilities developed so far. The technique can be further improved if bedform dynamics quantification is set as primary goal in the design of the technique's specifications.

This combination of techniques is fit for application in laboratory and field conditions. The rules of thumb described in the generation of the acoustic maps and the considerations on the spatial-temporal features of the data acquisition process, as related to the actual dynamics of the bedforms, are valid for both field and laboratory conditions. AMV is especially well suited and desirable for field data acquired with the increasingly popular acoustic technique for riverine environments, i.e., Acoustic Doppler Current Profilers and Multi-beam Echo-sounders. Targeting field implementation with this technique is of special importance as it provides a surrogate measurement that revolutionizes the way the bedload measurements are currently made.

## ACKNOWLEDGMENTS

We acknowledge the funding of Sándor Baranya from the Dr. Imre Korányi Scholarship and the János Bolyai fellowship of the Hungarian Academy of Sciences. Experiments for this research were conducted in a facility developed with funding from Iowa Department of Transportation. This support is gratefully acknowledged.

**REFERENCES**

Abraham, D. and Kuhnle, R. (2006). "Using High Resolution Data for Measuring Bed-Load Transport". Proceedings 8th Federal Interagency Sedimentation Conference, April 2-6, 2006, Reno, NV.

Adrian, R.J. (1991). "Particle-Imaging Techniques for Experimental Fluid Mechanics", *Ann Rev Fluid Mech*, (23), pp. 261-304.

Duffy, G. P. (2006). "Bedform Migration and Associated Sand Transport on a Banner Bank: Application of Repetitive Multibeam Surveying and Tidal Current Measurement to the Estimation of Sediment Transport", PhD Thesis. The University of New Brunswick.

Einstein, H.A. (1942). "Formulas for the transportation of bedload". *Transactions of the ASCE*, 107. 561-577

Fincham, A. M. and G.R. Spedding (1997). "Low-cost, High Resolution DPIV for Measurement in Turbulent Fluid Flows", *Exp. in Fluids*, 23, pp. 449-462

Friedrich, H., Melville, B.W., Coleman, S.E., Nikora, V. and Clunie, T.M. (2005) "Three-dimensional Measurement of Laboratory Submerged Bed Forms Using Moving Probes" 31rd IAHR, pp 396~404

Fujita, I., Muste, M. and Kruger, A. (1998). "Large-Scale Particle Image Velocimetry for Flow Analysis in Hydraulic Applications," *J. Hydr. Res.*, 36(3), pp. 397-414.

Gibb, J.P., Barcelona, M.J., Ritchey, J.D., LeFaivre, M.H. (1984). "Effective Porosity of Geologic Materials: First Annual Report. Champaign, Ill"; Illinois State Water Survey, SWS Contract Report 351.

Helley, E.J. and Smith, W. (1971). "Development and Calibration of a Pressure-difference Bedload Sampler," U.S. Geological Survery Open-file Report, 1-18.

Ho, H-C., Muste, M., Plenner, S., Firoozfar, A.R. (2012). "Laboratory Considerations for Supporting Multi-box Culvert Design," *Canadian Journal of Civil Engineering*, 40, dx.doi.org/10.1139/cjce-2012-0201, pp. 324-333.

Ho, H-C., Muste, M. and Ettema, R. (2013). "Sediment Self-cleaning Multi-box Culverts," *Journal of Hydraulic Research*, 51(1), pp. 92-101.

Kim, D., Muste, M., Merwade, V. (2015). "A GIS-based relational data model for multi-dimensional representation of river hydrodynamics and morphodynamics," *Environmental Modelling & Software*, 65, pp. 79-93.

Lin, C-Y.M. (2011). "Bedform Migration in Rivers," MSc Thesis, Simon Fraser University, Vancouver, BC, Canada

Muste M. and Ettema R. (2000). "River-Sediment Control at Conesville Station, on the Muskingum River, Ohio," IIHR *Report* No. 410, Iowa Institute of Hydraulic Research, The University of Iowa, Iowa City, IA

Muste, M., Fujita, I., and Hauet, A. (2008). Large-Scale Particle Image Velocimetry for Measurements in Riverine Environments, Special Issue on Hydrologic Measurements, *Water Resources Research*, 44, W00D19, doi: 10.1029/2008WR006950

Pal, D. and Gohsal, K. (2014). "Grain-size Distribution in Open Channel Flow by Mixing Length Approach," Environmetrics, DOI: 10.1002/env.2303.

Raffel, M., Willert, C.E., Kompenhans, J. (1998). "Particle Image VelocimetryL A Practical Guide," Springer, New York, NY. USA

Spasojevic, M. and Muste, M. (2002). Numerical model study of Berwick Harbor, Morgan City, Louisiana, IIHR—Hydroscience & Engineering Limited Distribution Report No. 422, IIHR—Hydroscience & Engineering, The University of Iowa, Iowa City, Iowa. U.S.A.

Simons, D.B., Richardson, E.V. and Nordin, C.F. (1965). "Bedload Equation for Ripples and Dunes," U.S. Geological Survey Professional Paper 463-H, pp. 1-9.

Van der Mark, C.F., Blom, A., Hulscher, S. (2008). "Quantification of variability in bedform geometry". Journal of Geophysical Research: Earth Surface 113 (F3).

Van Rijn, L.C. (1984). "Sediment Transport, Part I: Bed Load Transport". *Journal of Hydraulic Engineering*, ASCE, Vol. 110, No. 10